Selective regulation of calcium-permeable AMPA receptors by a novel TARP

David Soto[†], **Ian D. Coombs**[†], **Massimiliano Renzi**, **Marzieh Zonouzi**, **Mark Farrant**[*], and **Stuart G. Cull-Candy**[*]
Department of Neuroscience, Physiology and Pharmacology, University College London, Gower Street, London WC1E 6BT UK

Abstract

Although the properties and trafficking of AMPA-type glutamate receptors (AMPARs) depend critically on associated transmembrane AMPAR regulatory proteins (TARPs) such as stargazin (γ-2), no TARP has been described that can specifically regulate the important class of calcium-permeable (CP-) AMPARs. We examined the stargazin-related protein γ-5, which is highly expressed in Bergmann glia, a cell type possessing only CP-AMPARs. γ-5 was previously thought not to be a TARP, and it has been widely used as a negative control. Here we find that, contrary to expectation, γ-5 acts as a TARP and serves this role in Bergmann glia. Whereas, γ-5 interacts with all AMPAR subunits, and modifies their behavior to varying extents, its main effect is to regulate the function of AMPAR subunit combinations that lack short-form subunits, which constitute predominantly CP-AMPARs. Our results suggest an important role γ-5 in regulating the functional contribution of CP-AMPARs.

INTRODUCTION

Diversity in fast excitatory synaptic and neuron-glia signalling in the CNS arises, in part, from functional differences among AMPAR subtypes. Properties of individual AMPARs are dictated by their constituent subunits (GluR1-4), which function as homo- or heterotetrameric assemblies. Of these subunits, GluR2 is critical, being subject to posttranscriptional RNA editing which results in a glutamine-to-arginine (R) switch at the 'Q/R site' in its pore-lining region. This editing alters the properties of AMPARs, causing them to be calcium impermeable. By contrast, receptors that lack this subunit are permeable to calcium ions 1, 2, show a high single-channel conductance 3, and are blocked by endogenous intracellular polyamines 4-6. These features are critical in defining basic properties of excitatory transmission 7-9, and neuron-glia interaction 10. Although most AMPARs in the brain contain GluR2, and are therefore calcium-impermeable, there is growing evidence that the dynamic regulation of GluR2-lacking CP-AMPARs is key in neuron-glia signaling and in synaptic plasticity 9-13. Moreover such regulation has been implicated in aspects of neuronal development and in the etiology of debilitating neurological disorders 9,14,15. However, the way in which the surface expression and properties of CP-AMPARs are regulated remains unclear.

Since their discovery as integral components of AMPAR complexes in the CNS, TARPs have emerged as important molecular determinants of AMPAR behavior 16-18. Five TARPs have been identified – including the prototypical TARP, stargazin (γ-2). Each interacts with all four AMPAR subunits to shape central glutamate signaling by increasing single-channel

---

[*]Authors for correspondence: SGC-C: s.cull-candy@ucl.ac.uk MF: m.farrant@ucl.ac.uk.
[†]These authors contributed equally to this work.

conductance and channel open probability 19-23, decreasing polyamine block of calcium-permeable AMPARs (CP-AMPARs) 24, and regulating AMPAR trafficking 25-27. Although TARPs are crucial in AMPAR-mediated signaling, none have been described that are selective for CP-AMPARs or that control the properties of AMPARs in glia. The stargazin-related protein γ-5 has been widely used as a negative control in experiments with recognized TARPs 20, 21, 25. It does not rescue AMPAR responses in granule cells from γ-2-lacking stargazer mice 22, which lack γ-2 and is without the specific PDZ-binding domain through which other TARPs regulate AMPAR targeting 22,25,26. Given that γ-5 is intensely expressed in cerebellar Bergmann glia 28, and that neuron-glia signaling in these cells is dependent on CP-AMPARs 10,12,29,30, we considered whether γ-5 might modify CP-AMPARs. We found that γ-5 regulated selectively the functional properties of those AMPARs that lack short-form subunits, including AMPARs containing the GluR2Long (GluR2L) splice variant and homomeric CP-AMPARs composed of GluR1 or GluR4.

RESULTS

γ-5 modifies AMPAR properties

We determined properties of recombinant AMPARs expressed in tsA201 cells (see Methods) by studying currents evoked by rapid application of glutamate onto outside-out membrane patches (Fig. 1). Initially, we compared responses from cells transfected with GluR4 alone with those obtained from cells co-transfected with GluR4 and γ-5 (Fig. 1), or with recognized TARP family members (γ-2, γ-3, γ-4, γ-7 and γ-8) (Fig. 2). As expected 20, each of the established TARPs significantly increased single-channel conductance (estimated from non-stationary fluctuation analysis (NSFA); see Supplementary Table 1 online and Methods; Fig 2a). For example, with γ-2 transfection, conductance increased from 20.1 ± 1.3 pS to 31.4 ± 2.5 pS ($P = 0.0016$, $n = 8$ and 9 patches). We found that γ-5 produced a sizeable increase in single-channel conductance (from 20.1 ± 1.3 pS to 36.0 ± 2.6 pS; $P < 0.0001$, $n=8$ and 7 patches). The magnitude of the conductance increase seen with γ-5 was comparable to that obtained with each of the previously established TARP family members (all $P > 0.2$, $n = 5$ to 10) (Fig. 2a). Thus, contrary to previous expectations, γ-5 modified AMPAR behavior.

γ-5 behaves differently from other TARPs

To establish whether γ-5 regulated other functionally important AMPAR properties, we measured two parameters that contribute to the overall efficacy of the receptor population: the probability that agonist-bound channels will open (peak open probability, $P_{o,\text{peak}}$), and the speed of desensitization (τ_{des}). Whereas $P_{o,\text{peak}}$ for homomeric GluR4 AMPARs was not altered by expression together with the established TARPs, it was markedly decreased by γ-5 (from 0.57 ± 0.03 to 0.33 ± 0.03; $P < 0.0001$, $n = 8$ and 7) (Fig. 2b). Unlike γ-2, γ-3, γ-4 and γ-8 31-33, γ-5 did not slow receptor desensitization (3.47 ± 0.27 ms for GluR4 *vs* 3.01 ± 0.16 ms with γ-5, $P = 0.1731$, $n = 8$ and 7; this compares with 5.7 ± 0.7 ms for γ-2, $P = 0.0114$, $n = 9$) (Fig. 2c; see also 20,22. These observations suggested that γ-5 differed markedly from other TARPs in its influence on AMPARs. Of note, γ-7, the TARP family member whose sequence most closely resembles that of γ-5 22 did not slow desensitization either (3.47 ± 0.27 ms for GluR4 versus 3.27 ± 0.36 ms with γ-7; $P = 0.6525$, $n = 8$ and 5) (Fig. 2c).

We showed recently that the prototypical TARP, γ-2, attenuates the blocking action of intracellular polyamines on native and recombinant CP-AMPARs24, resulting in a decreased inward rectification. This property is shared by γ-5 (Fig 3a), which, like established TARPs, reduced rectification of homomeric GluR4 responses (quantified in Fig. 3b as the Rectification Index, $RI_{+60/-80}$; see Methods). Although significant, the effect of

γ-5 was less than that of other TARPs; this was also clear from the current versus voltage (*I-V*) plots comparing γ-5 and γ-3 (Fig. 3a), as well as from representative patch responses (Fig. 3c), where the relative peak and steady-state outward currents (at +80mV) were noticeably smaller with γ-5 than with γ-2 ($RI_{+60/-80}$ was 0.025 ± 0.003 for GluR4 versus 0.081 ± 0.012 with γ-5; $P = 0.0019$, $n = 5$ patches for both; this compares with 0.238 ± 0.032 with γ-2; $P = 0.0001$ versus γ-5, $n = 4$).

The effect of γ-5 on the functional properties of AMPARs was not restricted to homomeric GluR4. Coexpression of γ-5 also increased GluR1 single-channel conductance (from 19.6 ± 1.9 pS to 44.3 ± 4.2 pS, $P = 0.0002$; $n = 7$ and 6) and decreased $P_{o,peak}$ (from 0.53 ± 0.04 to 0.38 ± 0.03; $P = 0.015$), whereas τ_{des} was unchanged (2.3 ± 0.3 ms versus 2.3 ± 0.1ms, $P = 0.9967$) (Fig. 4). By contrast, γ-5 was without effect on single-channel conductance, $P_{o,peak}$, τ_{des} or RI of calcium-permeable GluR6(Q) kainate receptors (Fig. 4), indicating that its actions did not reflect a nonspecific modification of calcium-permeable receptors. Indirect effects of γ-5 also seem unlikely. Phosphorylation at Ser831 increases the single-channel conductance of homomeric GluR1 AMPARs [34]. As TARP gene family members can interact with voltage-gated calcium channels, γ-5 could conceivably facilitate the elevation of intracellular calcium, causing kinase activation, GluR1 phosphorylation and, ultimately, increased channel conductance. To test this, we made a GluR1 mutant (S831A) that was incapable of being phosphorylated. We found that γ-5 increased the conductance of GluR1 and $GluR1_{S831A}$ equally (from 16.2 ± 0.9 to 46.7 ± 5.6; $P = 0.00005$, n = 7 and 4 respectively), arguing against such indirect modulation.

CP-AMPARs in Bergmann glia are associated with γ-5

Is γ-5 involved in the regulation of native AMPARs? In the cerebellum, γ-5 is intensely expressed only in Bergmann glial cells (BGCs) [28], where it occurs with γ-4. BGCs have relatively uniform surface expression of CP-AMPARs, formed from GluR1 and/or GluR4 subunits [10,29,30,35]. To determine whether AMPARs in BGCs showed properties indicative of TARP association, we initially examined polyamine block using cells grown in primary culture (see Methods). The *I*-V plots obtained showed significantly less rectification than was seen with recombinant homomeric GluR1 or GluR4 assemblies expressed in the absence of a TARP (Supplementary Fig. 1 online), consistent with the idea that TARPs normally modify AMPARs in BGCs. We therefore next compared the properties of CP-AMPARs in outside-out patches from visually identified BGCs in acute cerebellar slices (Fig 5a) (see Methods), with those of recombinant AMPARs co-expressed with γ-4 or -5.

Following fast application of glutamate (10 mM, 100 ms) onto outside-out patches, we measured the kinetics of receptor desensitization (τ_{des}), and used NSFA to estimate single-channel conductance and $P_{o,peak}$ (Fig. 5b, c, d). For BGCs, τ_{des} was 2.54 ± 0.04 ms, $P_{o,peak}$ was 0.39 ± 0.03 and mean single-channel conductance was 35.7 ± 3.2 pS (all n = 8). For homomeric recombinant receptors, we obtained closely comparable values only when GluR4 subunits were expressed with γ-5 ($\tau_{des} = 3.0 \pm 0.2$, $P_{o,peak} = 0.33 \pm 0.03$, mean single-channel conductance 36.0 ± 2.6 pS, all n=7) (Fig. 5). When we compared the rectification of BGC AMPARs with that of recombinant AMPARs, once again we obtained equivalent values only when γ-5 was coexpressed ($RI_{+60/-60}$ for BGCs was 0.17 ± 0.03; for GluR4 plus γ-5 it was 0.15 ± 0.02; both n = 6) (see Fig. 5e). From these various measurements, it was clear that the properties of CP-AMPARs in BGCs differed substantially from those of recombinant GluR1 or GluR4 receptors expressed with or without γ-4, but that they matched well those of recombinant receptors assembled from GluR4 and γ-5. Indeed, of the receptors examined, this was the only combination between a homomeric AMPAR subunit and a TARP whose properties did not differ significantly from those of CP-AMPARs in BGCs. Of note, GluR1/GluR4 heteromeric receptors expressed with γ-5 also mimicked the properties of BGC AMPARs (conductance 29.2 ± 2.9 pS,

$P_{o,\text{peak}}$ 0.38 ± 0.07, τ_{des} 3.0 ± 0.2; all $n = 6$). Thus, irrespective of the GluR subunit(s) involved, CP-AMPARs in BGCs may be associated with γ-5.

Although this conclusion is drawn from recordings of somatic AMPARs in excised membrane patches from BGCs, two lines of evidence suggest that it may also apply to BGC AMPARs activated after release of glutamate from climbing and parallel fibres [36-38]. Recent experiments using double immunogold labeling [39] showed that the scaffolding protein SAP97 (Synapse-Associated Protein) is located with GluR1 in BGC plasma membrane facing parallel fiber synapses. In coimmunoprecipitation assays using whole cerebellar tissue from adult rat, we found an antibody to SAP97 interacted with both GluR1 and γ-5 (Fig. 6a) (see Methods). As γ-5 is found in the cerebellum only in CBGs, this finding strongly suggests that AMPARs, at points of contact between BGCs and parallel and climbing fibers, are associated with γ-5. A further coimmunoprecipitation assay confirmed that γ-5 also interacted with GluR4 in adult cerebellum, suggesting that both GluR1 and GluR4 may be associated with γ-5 at synaptic sites in BGCs (Fig 6a). As expected, a pan-TARP antibody also precipitated GluR4 from cerebellum, most likely reflecting the known interaction between stargazin and GluR4 in granule cells (Fig 6a). Next we compared published values for the decay of BGC quantal events[30], corrected from their higher recording temperature (see **Supplementary Methods** online), with the deactivation kinetics of recombinant receptors expressed with and without TARPs. In accord with our immunoprecipitation data suggesting the presence of γ-5, the decay of quantal events matched well with the deactivation kinetics of receptors expressed with γ-5 (Fig. 6b). Of note, the time constant for deactivation of GluR1 or GluR4 receptors expressed with γ-4 was more than five times that of the decay of BGC quantal events (Fig. 6c), suggesting that properties of AMPARs at points of contact with climbing and parallel fibers are determined by γ-5 rather than γ-4.

γ-5 differentially affects CP-AMPARs

If γ-5 is a TARP, why is it unable to rescue AMPAR surface expression or synaptic responses in *stargazer* cerebellar granule cells [22]? Lack of the amino acid motif–TTPV, which forms the PDZ-binding domain in other TARPS, may explain why γ-5 does not produce synaptic targeting, but, given our findings, it is surprising that no granule cell AMPAR surface expression is recovered in stargazer mutants. One possibility is that the effect of γ-5 on AMPAR-mediated macroscopic current shows subunit selectivity. To address this, we examined patches from tsA201 cells transfected with γ-5 and varying proportions of cDNA for GluR2 and GluR4. This allowed us to explore different AMPAR subtypes in a continuum of assemblies–from homomeric GluR4 to heteromeric GluR2/GluR4 (Fig. 7a).

As expected, we obtained a wide range of rectification values ($RI_{+60/-60}$; 0.07-1.35), reflecting the differing contribution of GluR2 subunits to AMPAR assemblies[1]. We plotted single-channel conductance as a function of RI, after grouping data according to whether patches showed a low (<0.4), intermediate (0.4–0.8) or high (>0.8) RI. For patches in which most receptors were expected to be homomeric GluR4 (transfected with a low proportion of GluR2 cDNA, and yielding a low RI), γ-5 produced a significant increase in single-channel conductance (from 13.4 ± 2.3 pS to 27.1 ± 2.6 pS; n = 8 and 7 respectively; $P = 0.0017$) (Fig. 7a). Similarly, conductance increased in patches with intermediate RI values (from 8.0 ± 0.8 pS to 15.4 ± 1.5 pS; n = 6 and 9; $P = 0.0023$). However, γ-5 had no significant effect on conductance for patches with a high RI (high proportion of heteromeric GluR2/GluR4 assemblies) (8.7 ± 1.1 pS with γ-5 versus 6.0 ± 1.1 pS without γ-5, n = 10 and 6; $P = 0.1303$). This suggested that γ-5 can selectively modify the properties of, or selectively

traffic, certain CP-AMPAR assemblies. This finding was unexpected, as no other TARP seems to be able to modify or deliver specific AMPAR subtypes.

γ-5 preferentially modifies long-form AMPARs

The selective action of γ-5 could require that the AMPAR assemblies lack GluR2 subunits, lack Q/R edited subunits, or lack short-form subunits (GluR2 and GluR3). To distinguish between these possibilities, we examined the effect of γ-5 on AMPARs containing GluR2L 40. Like GluR2, this naturally occurring splice variant is edited at the Q/R site in its pore-lining region, and hence suppresses AMPAR calcium permeability. However, in common with GluR1 and -4, it has a long C-tail 41. We transfected cells with GluR2L and GluR4 and estimated the single-channel conductance of high-RI patches (in which most AMPAR channels were expected to be heteromeric assemblies). These gave single-channel conductance estimates of 6.7 ± 1.0 pS (n = 6) in the absence of γ-5 and 14.2 ± 2.2 pS (n = 7; $P = 0.0143$) in the presence of γ-5. Thus, expression of γ-5 with GluR2L and GluR4 together gave a markedly increased single-channel conductance (Fig. 7a). The possibility that GluR2L itself gives rise to elevated conductance in high-RI patches can be excluded, as GluR2/4 and GluR2L/4 receptors both yielded very similar conductance estimates in the absence of γ-5 (Supplementary Table 2 online). Thus, the macroscopic properties of AMPARs may be modified by γ-5, irrespective of the presence of edited GluR2, provided the receptors are composed of long-form subunits.

We next compared the effects of γ-5 on unedited (Q) forms of GluR2 and GluR2L, to determine whether the γ-5-dependent modification of AMPAR properties was influenced by the calcium permeability of the assemblies *per se* (Fig. 7b–d and Supplementary Table 3 online). As a control, we examined the effects of γ-2, which increased the single-channel conductance of both GluR2(Q) (from 19.4 ± 1.3 to 30.5 ± 3.7 pS, $P = 0.0044$, n = 10 and 6) and GluR2L(Q) (from 17.7 ± 1.8 to 26.4 ± 2.3 pS, $P = 0.0129$, n = 7 and 6). By contrast, γ-5 increased conductance for GluR2L(Q) (to 33.0 ± 3.3 pS; $P = 0.0017$, n = 7) but produced a significant, though less marked, increase in the conductance of the unedited short-form GluR2(Q) (26.1 ± 1.8 pS; $P = 0.0066$; n = 8) (Fig. 7b). It is also of note that γ-5, unlike γ-2, did not increase the low $P_{o,peak}$ shown by homomeric GluR2Q (long or short) (Fig. 7c). It also changed RI only for the long forms (Fig. 7d), supporting the view that the action of γ-5 is preferentially seen with assemblies containing the long form of GluR2, independent of AMPAR calcium permeability.

According to our interpretation, established TARPs that are not subunit selective would be predicted to produce similar increases in single-channel conductance for GluR2/4 and GluR2L/4. As a control, we therefore compared the increase in single-channel conductance conferred by γ-2 on these AMPAR combinations (in patches with linear *I*–V plots) and demonstrated that this was indeed the case (γ-2 increased conductance of GluR2/4 to 11.1 ± 1.1 pS and GluR2L/4 to 14.4 ± 2.2 pS; n = 6 and 9; $P = 0.0213$ and $P = 0.0403$, respectively). A further prediction from the analysis in Figure 6a is that other short-form subunits will behave similarly to GluR2(short). We therefore examined the regulation of GluR3 by γ-5 and found that its channel conductance was increased, but again less so than that of long-form AMPARs (from 21.7 ± 2.6 to 31.2 ± 2.7; n = 9 and 12, respectively; $P = 0.0183$) (Fig. 7e).

To allow direct comparison with our GluR2(Q) data, and to test the prediction that γ-5 regulates Q and R forms similarly, we also measured channel properties of GluR2(R) homomers expressed with and without γ-5. As expected from previous single-channel recordings42, homomeric GluR2(R) AMPARs showed a relatively low single-channel conductance (5.1 ± 1.1 pS, n = 5); the conductance was not significantly increased by expression with γ-5 (6.5 ± 0.9, n = 9, $P = 0.3446$). It is apparent from a plot of conductance

versus $P_{o,\text{peak}}$ changes for homomeric and heteromeric receptors (Fig. 7e) that the influence of γ-5 on conductance was greatest when AMPARs lacked short-form subunits.

γ-5 influence on AMPAR surface expression

TARPs may bind to multiple regions of AMPAR subunits, including the extracellularly located flip-flop cassette23. It was thus of note that the selectivity of γ-5 seemed to depend on the length of the subunit's cytoplasmic tail. We therefore considered whether the relatively small effect of γ-5 on short-form subunits reflected a lack of binding or a lack of effective trafficking. To determine whether γ-5 bound to all AMPARs and, in particular, to both forms of GluR2 (long and short), we performed coimmunoprecipitation assays with a yellow fluorescent protein (YFP)–γ-5 construct (see Methods). Antibodies recognizing YFP were able to pull down both GluR2(Q) and GluR2L(Q) when these were expressed with YFP–γ-5 (Fig. 8a). Additionally, coimmunoprecipitation was obtained with homomeric GluR1 and GluR4, as well as with GluR2 when it was expressed in heteromeric GluR1/2(R), GluR2(R)/3 and GluR2(R)/4 combinations, indicating that these assemblies also interacted with γ-5 (data not shown). Given that GluR2 preferentially forms heteromers when expressed with other subunits, we have assumed that surface GluR2 in these conditions reflects heteromeric AMPARs. Together, our results indicate that γ-5 physically associates with the various AMPAR assemblies, regardless of their subunit composition or C-terminal length, consistent with the primary site of interaction being within the extracellular ligandbinding domain20,21.

If γ-5 interacts with GluR2-containing AMPAR-assemblies, does it alter their trafficking to the cell surface? To answer this, we used biotinylation to quantify total and cell-surface expression of GluR2(Q) protein. Cells were transfected with GluR2(Q) and green fluorescent protein (GFP; control) or with GluR2(Q) and YFP–γ-5. When GluR2(Q) was expressed with γ-5, its surface expression (percentage of total) was reduced from 66% ± 17% to 6% ± 3% (n = 3, $P = 0.0259$) (Fig. 8b,c). We extended these findings by examining the surface expression of GluR2L(Q) and GluR2R (Fig. 8c) and GluR1 and GluR4 (Supplementary Fig. 2 online). In no case was surface expression increased, and that of GluR2(Q) and GluR2L(Q) was significantly decreased.

For comparison with biotinylation data, we also recorded whole-cell currents for homomeric GluR2(Q), GluR2L(Q) and GluR2(R) receptors with and without γ-5 (see Methods). γ-5 significantly decreased the glutamate-evoked steady-state current for cells expressing GluR2(Q) (Fig. 8d; from 33.8 ± 9.8 to 6.9 ± 1.9 pA pF^{-1}, n = 8 and 6, respectively; $P = 0.0374$) or GluR2L(Q) (from 36.0 ± 6.6 pA pF^{-1} to 8.3 ± 2.2 pA pF^{-1}, n = 8 and 7 respectively, $P = 0.0011$). Conversely, with homomeric GluR2(R) the current density was increased (from 27.1 ± 10.9 to 65.9 ± 17.9 pA pF^{-1}, n = 7 and 6, respectively; $P = 0.0281$). To confirm the validity of this approach as an assay of surface expression, we measured rates of desensitization and resensitization and recorded steady-state currents in excised patches containing GluR2(Q) expressed with and without γ-5 (see Supplementary Fig. 3 online for details). Together our data indicate that γ-5 is able to decrease the surface expression of certain GluR2-containing AMPARs, but unlike the effects on receptor properties, the decrease in surface expression is not solely dependent on AMPAR C-tail length. In support of this, we also observed a decrease in current density with GluR2L(R). Together, these results suggest that surface expression of GluR2 homomers is decreased, except when the subunit is of the edited short form. The decrease seems specific for γ-5, as the current density for GluR2(Q) and GluR2L(Q) was increased by the closely related TARP γ-7 (from 33.8 ± 9.7 to 302.4 ± 75.3 pA pF^{-1}; n = 8 and 5, respectively; $P = 0.0008$; and from 36.0 ± 6.6 to 112.7 ± 30.3 pA pF^{-1}; n = 8 and 4; $P = 0.0066$).

Why are the functional properties of AMPARs that contain short-form subunits differentially modulated, given that γ-5 can bind to these receptors? Either the binding of γ-5 to these subunits only weakly modifies their properties, or most of those AMPARs that reach the cell surface are 'TARPless'. In the former case, one would expect a homogenous population of channels, whereas in the latter, one would expect a heterogeneous population of conductances, corresponding to 'TARPed' and 'TARPless' receptors. To address the question of whether expression of any AMPAR subunit together with γ-5 can result in heterogeneous receptor assembly, we examined a subset of patches in which we could compare NSFA data with channel conductance estimates from all-point amplitude histograms of resolved events (Supplementary Fig. 4 online). Although one would not anticipate identical values from the two methods, a reasonable correspondence would be expected if patches from cells transfected with γ-5 contained a homogeneous channel population, whereas a poor correspondence would be expected if patches contained some resolvable large-conductance openings from TARPed receptors, together with low-conductance brief openings associated with TARPless AMPARs (see ref. 20). In four patches from cells expressing GluR1 and γ-5, the two methods gave estimates that were reasonably comparable (~35 and 45 pS; Supplementary Fig. 4). The same analyses with GluR2(Q) plus γ-5 gave single-channel conductance estimates of ~27 and 38 pS (three patches). Together, these results suggest broadly homogeneous channel populations. Thus, although we do not exclude the possibility of some TARPless channels, most AMPARs in the patches examined are likely to be associated with γ-5.

Previously, it has been shown that chimeric γ-5 bearing the cytoplasmic tail of stargazin can facilitate AMPAR surface expression[20], suggesting a pivotal role for this domain in AMPAR modulation. We therefore made a truncated form of γ-5 without an intracellular tail (γ-5$_{1–206}$) and examined its effect on homomeric GluR2(Q) receptors. Unlike full-length γ-5 which produced a small increase in channel conductance (Fig. 7b), the truncated γ-5$_{1–206}$ increased conductance (to 36.2 ± 2.2 pS, n = 5, $P < 0.0001$ versus GluR2(Q) alone; $P = 0.0095$ versus GluR2(Q) with γ-5). These results indicate that the C-tail of γ-5 affects the degree to which channel conductance is enhanced. This suggests that either the C-tail itself positively influences the conductance change (see also ref. 21) but is less effective in short forms, or that other regions of γ-5 drive the conductance increase and this action is inhibited by the C-tail when γ-5 is associated with shortform AMPARs.

DISCUSSION

Our experiments establish that γ-5 is a functionally active member of the stargazin family of TARPs. We found that, in common with established TARPs, γ-5 could increase single-channel conductance, regulate channel behavior and reduce sensitivity to block by endogenous intracellular polyamines (see refs. 20–25). The fact that the role of γ-5 was previously overlooked can be readily accounted for by our finding that γ-5 shows properties that are fundamentally different from other TARPs. First, although γ-5 modifies, to varying extents, channel properties of all AMPAR assemblies, its main effect is to regulate those channels composed of long-form subunits (GluR1, GluR4 and GluR2L). With the exception of GluR2L-containing assemblies, these AMPARs are calcium-permeable subtypes. Second, unlike established TARPs [43], γ-5 reduces or does not increase the surface expression of AMPARs. Third, γ-5 differs from all other TARPs in decreasing the open probability of AMPAR channels.

As surface expression of recombinant AMPARs can be decreased or unchanged and $P_{o,peak}$ reduced, γ-5 might be thought to serve a generally suppressive function. However, it remains to be determined precisely how γ-5 operates in the presence of other trafficking and regulatory proteins present in glia and neurons. The PDZ binding domains of γ-5, and of its

close relative γ-7, differ from those of other TARPs, suggesting that they may interact with distinct protein partners26. Both have unusually short C-tails and, consequently, lack all but two of the ten phosphorylation sites present in the C-tails of other TARPs. As these sites are thought to be involved in regulation of AMPAR trafficking44,45, it seems likely these differences between TARPs could enable differential receptor regulation.

Although γ-5 does not enhance AMPAR surface expression, our experiments indicate it increases current density of homomeric AMPARs composed of the common short-form GluR2(R) subunit. As this increase in membrane current occurs without a significant change in single-channel conductance, it seems likely that channel gating is altered. This emphasizes that γ-5 is capable of modifying functional properties of short-form AMPARs. The small responses obtained from GluR2(R) patches precluded a detailed functional investigation. However, a change in gating is of interest, as certain well studied neuronal cell types are thought to express a significant proportion of GluR2(R) homomers46.

Within the cerebellum, only BGCs express γ-5 mRNA28. These cells express CP-AMPARs that are involved in neuron–glia signaling47 and are crucial for the maintenance of normal synaptic transmission from parallel and climbing fibers to Purkinje cells10,39. Despite the importance of AMPARs in neuron–glia interplay, it was previously unknown whether TARPs influence the trafficking, anchoring or functional properties of AMPARs in glia, as they do in neurons. Our experiments indicate that CP-AMPARs in these cells have properties that match well those shown by recombinant γ-5–associated AMPARs. Furthermore, our data indicate that the properties of GluR4/γ-5 assemblies match those of the unitary currents activated during neuron–glia signaling in BGCs. The plasma membrane of BGCs directly facing sites of ectopic glutamate release from climbing and parallel fibers contains both SAP97 and GluR subunits39. As γ-5 in the cerebellum is restricted to BGCs, our finding that γ-5 antibody pulls down SAP97 supports these previous observations. Together, our data suggest that γ-5 is associated with AMPARs in the BGC membrane apposed to presynaptic terminals, and that it determines the properties of the CP-AMPARs underlying neuron–BGC signaling. This is a critical issue, as calcium signaling in glia (including astrocytes, oligodendrocytes and BGCs) is known to influence their morphology, function48 and survival13–and continuous activation of BGC CP-AMPARs, by glutamate released from climbing and parallel fibers30, is essential for maintenance of connections to Purkinje cells10.

γ-5 is present in the olfactory bulb, globus pallidus, hippocampal CA2 region and thalamus28, where it would be expected to regulate AMPAR-mediated calcium entry. The inability of γ-5 to 'rescue' of AMPAR responses in TARP-lacking cerebellar granule cells from stargazer mice22,49 is entirely consistent with our findings. Granule cells express predominantly the short-form subunits GluR2 and GluR4c. We found only a small increase in channel conductance when GluR2/GluR4 heteromers were coexpressed with γ-5; this, together with the fact that γ-5 does not enhance AMPAR surface expression, suggests γ-5 is unlikely to alter the macroscopic current in granule cells.

While our manuscript was in revision, a paper was published50 also showing that γ-5 is a TARP with subunit selectivity. However, that study differs notably from our own in concluding that only GluR2-containing (calcium-impermeable) AMPARs are regulated by γ-5, that this specificity depends on editing at the Q/R site of GluR2, and that γ-5 does not control receptor trafficking or surface expression of AMPARs. Although we found, in one case (homomeric GluR2 AMPARs), that γ-5 had apparent editing-dependent effects, these recent findings50 contrast with our main conclusion: that γ-5 interacts with all AMPAR subunits and, to varying extents, modifies their properties. In our studies, the predominant functional effect of γ-5 was on long-form AMPARs, which (with the exception of the splice

variant GluR2L) are calcium permeable. We found that this selectivity of γ-5 was not dependent on the Q/R editing state. The presence and function of γ-5 in BGCs, a cell type that expresses only CP-AMPARs29, seems inconsistent with the view that this TARP affects only GluR2-containing AMPARs. The reasons for these apparent discrepancies remain to be determined. However, our data indicate that the γ-5-induced increase in current for R but not Q forms of homomeric GluR2 AMPARs, rather than reflecting selectively enhanced function of edited receptors, results in part from reduced surface expression of GluR2Q. Furthermore, whole-cell recordings50 did not show γ-5 regulation of long-form CP-AMPARs, which could be explained by our finding that a doubling in single-channel conductance of γ-5–associated receptors is counteracted by a reduced probability of channel opening.

METHODS

Heterologous expression

We expressed recombinant receptors in tsA201 cells (derived from HEK293 cells stably transfected with the temperaturesensitive gene for SV40 T-antigen), as previously described24. Further details are presented in the **Supplementary Methods**. AMPAR subunit cDNAs (rat, flip isoforms) were gifts from S. Heinemann and P. Seeburg. TARP cDNAs (rat; γ-2, γ-3, γ-4, γ-5 and γ-8) were gifts from R. Nicoll. Human γ-7 cDNA was from OriGene Technologies Inc.

Fast agonist application to excised patches

We recorded macroscopic currents at 22–25 °C from outside-out patches (low-pass filtered at 10 kHz and digitized at 20 or 50 kHz), as previously described24. The 'external' solution contained (in mM) 145 NaCl, 2.5 KCl, 1 $CaCl_2$, 1 $MgCl_2$, 10 glucose and 10 HEPES buffer, pH 7.3 with NaOH. Rapid application of glutamate (1 or 10 mM) and, where indicated, cyclothiazide (50 μM; Tocris) was achieved by piezoelectric translation of an application tool24. The 'internal' (pipette) solution contained (in mM) 145 CsCl, 2.5 NaCl, 1 cesium EGTA, 4 Mg-ATP, 10 HEPES, pH 7.3 with CsOH and 0.1 spermine tetrahydrochloride (Tocris). We used NSFA to deduce channel properties from macroscopic responses24. Further details are presented in the Supplementary Methods. The rectification index (RI) was defined as the ratio of average peak current responses at +60 mV divided by the response at −80 mV (I+60mV/I−80mV). Elsewhere (Supplementary Fig. 1; Fig. 5e) RI was measured similarly, although the negative voltage used was −60 mV. Thus, RI values were directly comparable within, but not across, different experiments.

Whole-cell recordings

tsA201 cells were transfected with AMPAR subunit cDNA and either γ-5 or EGFP (control) cDNA. After 24 h, we replated cells onto coverslips. After a further 24 h, we made whole-cell recordings from isolated cells (thick-walled 4–7 MO electrodes; final series resistance 8–18 MO, subsequently compensated by 70%, 7-ms lag). The pipette solution was as above. A ramp protocol was used to change the holding potential (0, −70, +60 mV at a rate of 162.5 mV s□1, with the voltage held at −70 mV for 200 ms). Records were filtered at 2 kHz and sampled at 5 kHz. Receptors were activated by a bath application of 1 mM glutamate. We subtracted control traces from stable agonist-activated responses and measured the average current at −70 mV. To control for possible differences in cell surface area, we normalized the response by the input capacitance (pA/pF; where capacitance measured from the amplifier was 8–26 pF).

AMPAR deactivation kinetics and BGC quantal event decay constants

We measured AMPAR deactivation in response to 1-ms applications of 1 mM glutamate in the presence of 50 μM cyclothiazide (Fig. 6b). The current decay was fitted with a double exponential. After correction for temperature differences (see **Supplementary Methods**), the kinetics were compared with the decay time constants of quantal events previously[30] recorded from BGCs (Fig. 6c).

Coimmunoprecipitation from brain

We homogenized cerebellar tissue from three rats in buffer A (50 mM Tris-HCl, 0.5% Triton X-100, 150 mM NaCl, 1 mM phenylmethylsulfonyl fluoride, 1 mM EDTA, and protease inhibitor cocktail; Roche) and solubilized it for 1 h at 4 °C. Tissue was centrifuged (50,000g, 45 min, 4 °C) and the lysate incubated overnight with 1 mg of antibody to γ-5 (anti–γ-5; Sigma-Aldrich). After 24 h, the lysate was incubated with 20 ml of protein G–Sepharose (Sigma; 1 h, 4 °C). The protein G pellet was washed three times in buffer A. Adherent protein was separated on an SDS gel. The proteins were transferred onto nitrocellulose and blotted with anti-SAP97 (1:100) or anti-GluR4 (1:100; both Santa Cruz Biotechnology). As internal controls, we also incubated lysates with either pan-TARP (γ-2, γ-3, γ-4, γ-8) antibody or anti-GluR1 (both Millipore).

Coimmunoprecipitation of heterologously expressed receptors

tsA201 cells were grown in flasks and transfected with equal amounts of AMPAR and YFPγ-5 cDNA. After 24 h, we washed cells with PBS and lysed them in TNE buffer (50 mM Tris-HCl, pH, 8.0, 150 mM NaCl, 1 mM EDTA, 0.5% Triton X-100 plus protease inhibitor cocktail (Roche)) for 1 h. After centrifugation (10 min, 14,000g), we removed an aliquot to serve as the input protein sample and incubated the remaining lysate with 1 mg of rabbit anti-GFP (Invitrogen) or rabbit IgG control. After 24 h, we incubated lysates (1 h, 4 °C) with 20 ml of protein G (Sigma). Bound proteins were eluted with SDS sample buffer by boiling (5 min, 95 °C). Immunoprecipitated samples and cell lysates were separated by SDS-PAGE followed by western blotting with mouse anti-GluR2 or rabbit anti-GluR1 (Chemicon; Millipore UK) and anti-GFP (Invitrogen).

Cell surface biotinylation of AMPARs

tsA201 cells were transfected with cDNA for AMPAR subunits and either GFP (as control) or γ-5. After 24 h, we chilled the cells on ice and washed them twice with ice-cold PBS containing 1 mM $MgCl_2$, 2.5 mM $CaCl_2$. The cells were then treated (20 min on ice) with 1 mg ml^{-1} sulfo-NHS-biotin (Pierce). Unreacted biotinylation reagent was quenched by washing the cells three times for 5 min with 50 mM glycine in PBS containing Mg^{2+} and Ca^{2+}, followed by two washes in ice-cold PBS containing Mg^{2+} and Ca^{2+}. Cells were harvested in RIPA buffer (Perbio) and solubilized by rotating (1 h, 4 °C). Homogenates were centrifuged (14,000g, 10 min, 4 °C) and the input aliquot removed. The remaining supernatant was incubated (3 h, 4 °C) with 20 ml of 50% UltraLink Immobilized NeutrAvidin Protein (Pierce). After incubation, the NeutrAvidin protein was washed twice with high-NaCl RIPA buffer (500 mM NaCl) and once with low-NaCl RIPA (150 mM NaCl), and bound proteins were eluted with SDS sample buffer by boiling (5 min, 95 1C). Western blotting was carried out using an XCell SureLoc Novex Mini-Cell system (Invitrogen). The biotinylated proteins were probed using antibodies to GluR1, GluR2 and GluR4 (Chemicon). Immunoblots were visualized by ECL development (GE Healthcare Life Sciences) and quantified on a calibrated densitometer (Bio-Rad GS-800).

Dissociated cell culture

We obtained mixed cultures of cerebellar neurons and glia from newborn (postnatal days (P) 1–6) male and female C57BL/6 mice. All procedures were in accordance with the UK Animals (Scientific Procedures) Act 1986. Briefly, after decapitation, we removed brains and aseptically isolated the cerebella at 0.5–4 °C before mechanical dissociation. Cultures were plated (1×10^6 cells per 25 cm^2) and grown (37 °C, 5% CO_2) on poly-L-lysine–coated coverslips in basal Eagle's medium supplemented with 10% endotoxin-free fetal calf serum, 2 mM glutamine and 100 mg ml^{-1} gentamicin. After 1–14 d in vitro, coverslips were transferred to a submerged recording chamber, perfused with tsA201 'external' solution at room temperature (22-25 °C) and viewed under phase contrast optics. We identified BGC from their elongated or fusiform shape and whole-cell capacitance (12 ± 2 pF, n = 14) [29]. Whole-cell recordings were made (as for tsA201 cells) with voltage ramps (162.5 mV ms^{-1}) from −70 to +60 mV. Currents were low-pass filtered at 1 kHz and digitized at 2 kHz. Records obtained in glutamate (1 mM, plus 5–50 µM cyclothiazide) were leak-subtracted using control records. No liquid junction potential corrections were made. Rectification index was defined as the value of I_{+60mV}/I_{-60mV}. No difference was noted between cells maintained for different numbers of days in vitro, and we pooled the data.

Acute cerebellar slices

C57BL/6 mice (P34–49) were anesthetized with isoflurane and decapitated. We cut parasagittal slices (250 mm) from the cerebellar vermis, as previously described [24]. Slices were transferred to a submerged recording chamber at room temperature, perfused (1.5–2.5 ml min^{-1}) with 'external' solution (containing, in mM, 125 NaCl, 2.5 KCl, 2 CaCl2, 1 MgCl2, 25 NaHCO3, 1.25 NaH2PO4 and 25 glucose, pH 7.4 when bubbled with 95% O_2 and 5% CO_2) and visualized under infrared differential interference contrast optics. BGCs were identified by their position (proximal to Purkinje cells' somata), morphology and electrophysiological properties (input capacitance 35 ± 3 pF, n = 12) [37]. Pipettes were made from thin-walled borosilicate glass tubing (1.5 mm outer diameter, 1.17 mm inner diameter; G150TF-3; Warner Instr.), coated with Sylgard resin (Dow Corning 184) and fire polished to a resistance of 10 MΩ. The 'intracellular' (pipette) solution was the same as for tsA201 recordings. Recordings were filtered at 10 kHz and digitized at 50 kHz. All experiments were made in the presence of 1 µM strychnine hydrochloride, 20 µM SR-95531, 1 µM tetrodotoxin and 50 µM D-2-amino-5-phosphonopentanoate. The activation of metabotropic glutamate receptors was prevented by perfusion of 50 µM LY367385 starting at least 5 min before and continuing throughout the recording. Fast application of glutamate to excised patches and NSFA were performed as for tsA201 cells.

Statistics

Statistical analysis was performed using PRISM (GraphPad Software), with a two-tailed, unpaired Student's t-test or (when data were non-normally distributed; Shapiro-Wilk normality test) a Mann-Whitney U-test. Differences were considered significant at P < 0.05.

Supplementary Material

Refer to Web version on PubMed Central for supplementary material.

Acknowledgments

References

1. Geiger JR, et al. Relative abundance of subunit mRNAs determines gating and Ca^{2+} permeability of AMPA receptors in principal neurons and interneurons in rat CNS. Neuron. 1995; 15:193–204. [PubMed: 7619522]

2. Seeburg PH, Hartner J. Regulation of ion channel/neurotransmitter receptor function by RNA editing. Curr. Opin. Neurobiol. 2003; 13:279–283. [PubMed: 12850211]

3. Swanson GT, Kamboj SK, Cull-Candy SG. Single-channel properties of recombinant AMPA receptors depend on RNA editing, splice variation, and subunit composition. J. Neurosci. 1997; 17:58–69. [PubMed: 8987736]

4. Bowie D, Mayer ML. Inward rectification of both AMPA and kainate subtype glutamate receptors generated by polyamine-mediated ion channel block. Neuron. 1995; 15:453–462. [PubMed: 7646897]

5. Kamboj SK, Swanson GT, Cull-Candy SG. Intracellular spermine confers rectification on rat calcium-permeable AMPA and kainate receptors. J. Physiol. 1995; 486:297–303. [PubMed: 7473197]

6. Koh DS, Burnashev N, Jonas P. Block of native Ca^{2+}-permeable AMPA receptors in rat brain by intracellular polyamines generates double rectification. J. Physiol. 1995; 486:305–312. [PubMed: 7473198]

7. Bowie D, Lange GD, Mayer ML. Activity-dependent modulation of glutamate receptors by polyamines. J. Neurosci. 1998; 18:8175–8185. [PubMed: 9763464]

8. Rozov A, Burnashev N. Polyamine-dependent facilitation of postsynaptic AMPA receptors counteracts paired-pulse depression. Nature. 1999; 401:594–598. [PubMed: 10524627]

9. Cull-Candy S, Kelly L, Farrant M. Regulation of Ca^{2+} -permeable AMPA receptors: synaptic plasticity and beyond. Curr. Opin. Neurobiol. 2006; 16:288–297. [PubMed: 16713244]

10. Iino M, et al. Glia-synapse interaction through Ca2+ -permeable AMPA receptors in Bergmann glia. Science. 2001; 292:926–929. [PubMed: 11340205]

11. Ge WP, et al. Long-term potentiation of neuron-glia synapses mediated by Ca2+-permeable AMPA receptors. Science. 2006; 312:1533–1537. [PubMed: 16763153]

12. Matsui K, Jahr CE. Exocytosis unbound. Curr. Opin. Neurobiol. 2006; 16:305–311. [PubMed: 16675216]

13. Gallo V. Surprising synapses deep in the brain. Nat. Neurosci. 2007; 10:267–269. [PubMed: 17318215]

14. Bellone C, Luscher C. Cocaine triggered AMPA receptor redistribution is reversed in vivo by mGluR-dependent long-term depression. Nat. Neurosci. 2006; 9:636–641. [PubMed: 16582902]

15. Kwak S, Weiss JH. Calcium-permeable AMPA channels in neurodegenerative disease and ischemia. Curr. Opin. Neurobiol. 2006; 16:281–287. [PubMed: 16698262]

16. Kristensen AS, Traynelis SF. Neuroscience: an intrusive chaperone. Nature. 2005; 435:1042–1043. [PubMed: 15973396]

17. Nicoll RA, Tomita S, Bredt DS. Auxiliary subunits assist AMPA-type glutamate receptors. Science. 2006; 311:1253–1256. [PubMed: 16513974]

18. Osten P, Stern-Bach Y. Learning from stargazin: the mouse, the phenotype and the unexpected. Curr. Opin. Neurobiol. 2006; 16:275–280. [PubMed: 16678401]

19. Priel A, et al. Stargazin reduces desensitization and slows deactivation of the AMPA-type glutamate receptors. J. Neurosci. 2005; 25:2682–2686. [PubMed: 15758178]

20. Tomita S, et al. Stargazin modulates AMPA receptor gating and trafficking by distinct domains. Nature. 2005; 435:1052–1058. [PubMed: 15858532]

21. Turetsky D, Garringer E, Patneau DK. Stargazin modulates native AMPA receptor functional properties by two distinct mechanisms. J. Neurosci. 2005; 25:7438–7448. [PubMed: 16093395]

22. Kato AS, et al. New transmembrane AMPA receptor regulatory protein isoform, gamma-7, differentially regulates AMPA receptors. J. Neurosci. 2007; 27:4969–4977. [PubMed: 17475805]

23. Ziff EB. TARPs and the AMPA Receptor Trafficking Paradox. Neuron. 2007; 5:627–633. [PubMed: 17329203]

24. Soto D, Coombs ID, Kelly L, Farrant M, Cull-Candy SG. Stargazin attenuates intracellular polyamine block of calcium-permeable AMPA receptors. Nat. Neurosci. 2007; 10:1260–1267. [PubMed: 17873873]

25. Tomita S, Fukata M, Nicoll RA, Bredt DS. Dynamic interaction of stargazin-like TARPs with cycling AMPA receptors at synapses. Science. 2004; 303:1508–1511. [PubMed: 15001777]

26. Bats C, Groc L, Choquet D. The Interaction between Stargazin and PSD-95 Regulates AMPA Receptor Surface Trafficking. Neuron. 2007; 5:719–734. [PubMed: 17329211]

27. Matsuda S, et al. Accumulation of AMPA receptors in autophagosomes in neuronal axons lacking adaptor protein AP-4. Neuron. 2008; 57:730–745. [PubMed: 18341993]

28. Fukaya M, Yamazaki M, Sakimura K, Watanabe M. Spatial diversity in gene expression for VDCCgamma subunit family in developing and adult mouse brains. Neurosci. Res. 2005; 53:376–383. [PubMed: 16171881]

29. Burnashev N, et al. Calcium-permeable AMPA-kainate receptors in fusiform cerebellar glial cells. Science. 1992; 256:1566–1570. [PubMed: 1317970]

30. Matsui K, Jahr CE, Rubio ME. High-concentration rapid transients of glutamate mediate neural-glial communication via ectopic release. J. Neurosci. 2005; 25:7538–7547. [PubMed: 16107641]

31. Cho CH, St-Gelais F, Zhang W, Tomita S, Howe JR. Two families of TARP isoforms that have distinct effects on the kinetic properties of AMPA receptors and synaptic currents. Neuron. 2007; 55:890–904. [PubMed: 17880893]

32. Korber C, Werner M, Kott S, Ma ZL, Hollmann M. The transmembrane AMPA receptor regulatory protein gamma 4 is a more effective modulator of AMPA receptor function than stargazin (gamma 2). J. Neurosci. 2007; 27:8442–8447. [PubMed: 17670991]

33. Milstein AD, Zhou W, Karimzadegan S, Bredt DS, Nicoll RA. TARP subtypes differentially and dose-dependently control synaptic AMPA receptor gating. Neuron. 2007; 55:905–918. [PubMed: 17880894]

34. Derkach V, Barria A, Soderling TR. Ca2+/calmodulin-kinase II enhances channel conductance of α-amino-3-hydroxy-5-methyl-4-isoxazolepropionate type glutamate receptors. Proc. Natl. Acad. Sci. USA. 1999; 96:3269–3274. [PubMed: 10077673]

35. Wisden W, Seeburg PH. Mammalian ionotropic glutamate receptors. Curr. Opin. Neurobiol. 1993; 3:291–298. [PubMed: 8396474]

36. Bergles DE, Dzubay JA, Jahr CE. Glutamate transporter currents in Bergmann glial cells follow the time course of extrasynaptic glutamate. Proc. Natl. Acad. Sci. USA. 1997; 94:14821–14825. [PubMed: 9405697]

37. Clark BA, Barbour B. Currents evoked in Bergmann glial cells by parallel fibre stimulation in rat cerebellar slices. J. Physiol. (Lond.). 1997; 502:335–350. [PubMed: 9263914]

38. Matsui K, Jahr CE. Ectopic release of synaptic vesicles. Neuron. 2003; 40:1173–1183. [PubMed: 14687551]

39. Douyard J, Shen L, Huganir RL, Rubio ME. Differential neuronal and glial expression of GluR1 AMPA receptor subunit and the scaffolding proteins SAP97 and 4.1N during rat cerebellar development. J. Comp. Neurol. 2007; 502:141–156. [PubMed: 17335044]

40. Kolleker A, et al. Glutamatergic plasticity by synaptic delivery of GluR-B(long)-containing AMPA receptors. Neuron. 2003; 40:1199–1212. [PubMed: 14687553]

41. Kohler M, Kornau HC, Seeburg PH. The organization of the gene for the functionally dominant alpha-amino-3-hydroxy-5-methylisoxazole-4-propionic acid receptor subunit GluR-B. J. Biol. Chem. 1994; 269:17367–17370. [PubMed: 7545935]

42. Swanson GT, Feldmeyer D, Kaneda M, Cull-Candy SG. Effect of RNA editing and subunit co-assembly single-channel properties of recombinant kainate receptors. J. Physiol. (Lond.). 1996; 492:129–142. [PubMed: 8730589]

43. Yamazaki M, et al. A novel action of stargazin as an enhancer of AMPA receptor activity. Neurosci. Res. 2004; 50:369–374. [PubMed: 15567474]

44. Choi J, et al. Phosphorylation of stargazin by protein kinase A regulates its interaction with PSD-95. J. Biol. Chem. 2002; 277:12359–12363. [PubMed: 11805122]

45. Tomita S, Stein V, Stocker TJ, Nicoll RA, Bredt DS. Bidirectional synaptic plasticity regulated by phosphorylation of stargazin-like TARPs. Neuron. 2005; 45:269–277. [PubMed: 15664178]

46. Lee SH, Simonetta A, Sheng M. Subunit rules governing the sorting of internalized AMPA receptors in hippocampal neurons. Neuron. 2004; 43:221–236. [PubMed: 15260958]

47. Piet R, Jahr CE. Glutamatergic and purinergic receptor-mediated calcium transients in Bergmann glial cells. J. Neurosci. 2007; 27:4027–4035. [PubMed: 17428980]

48. Ziskin JL, Nishiyama A, Rubio M, Fukaya M, Bergles DE. Vesicular release of glutamate from unmyelinated axons in white matter. Nat. Neurosci. 2007; 10:321–330. [PubMed: 17293857]

49. Chen L, et al. Stargazin regulates synaptic targeting of AMPA receptors by two distinct mechanisms. Nature. 2000; 408:936–943. [PubMed: 11140673]

50. Kato AS, Siuda ER, Nisenbaum ES, Bredt DS. AMPA receptor subunit-specific regulation by a distinct family of type II TARPs. Neuron. 2008; 59:986–996. [PubMed: 18817736]
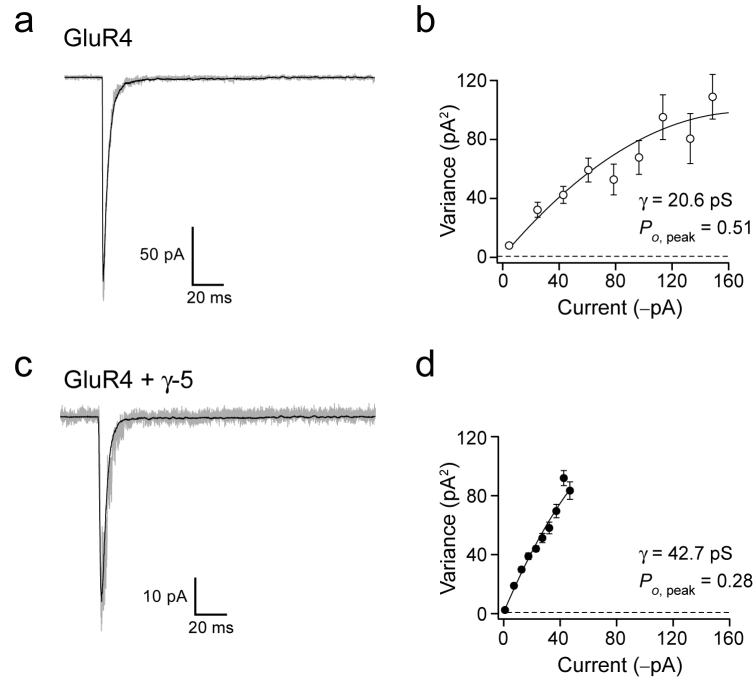
Figure 1. γ-5 modifies GluR4 conductance and $P_{o,peak}$
(**a–d**) Currents, and associated current-variance plots, evoked by rapid application of 10 mM glutamate (100 ms, −60 mV) to outside-out patches from tsA201 cells expressing homomeric GluR4 AMPARs (**a**) or GluR4 plus γ-5 (**c**). Solid lines are means of 25 traces without γ-5 and 135 traces with γ-5; gray lines show representative raw traces. Current–variance relationships (same scaling) generated from the recordings shown in **a** and **c** are given in **b** and **d**, respectively. For these two patches, the fitted parabola (see Methods) gave estimates of weighted mean single-channel conductance (g) of 20.6 pS and $P_{o,peak}$ of 0.51 for GluR4 alone; for GluR4 plus γ-5, the corresponding values were 42.7 pS and 0.28, respectively. Dashed lines denote background variance.
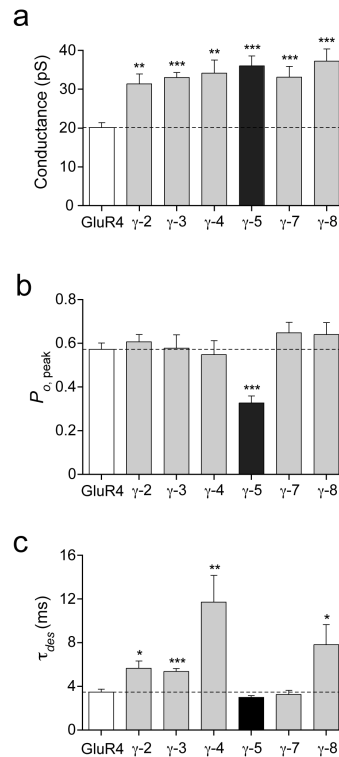
Figure 2. γ-5 shows unusual TARP-like features
(**a–c**) Bar graphs comparing the effect of the different TARPs (γ-5, black; other TARPs, gray; no TARP, white) on estimated mean single-channel conductance (**a**), probability of agonist-bound channel opening (peak open probability, $P_{o,peak}$; **b**) and kinetics of receptor desensitization (τ_{des}) of homomeric GluR4 receptors (**c**). Error bars, s.e.m.; *$P < 0.05$; **$P < 0.005$; ***$P < 0.0005$; see Supplementary Table 1.
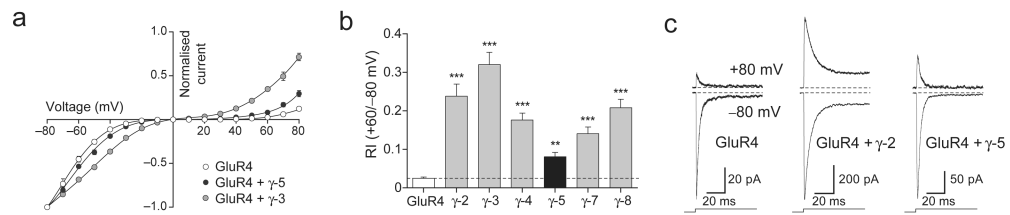
Figure 3. γ-5 affects AMPAR rectification

(**a**) Inwardly rectifying *I*–V relationships for peak currents evoked by glutamate (10 mM, 100 ms) applied to outside-out patches from tsA201 cells containing homomeric AMPARs formed from GluR4 alone (n = 5), GluR4 with γ-3 (n = 4) or GluR4 with γ-5 (n = 5). The intracellular solution contained 100 mM spermine. Currents are normalized to values at −80 mV; error bars, s.e.m.; solid lines, fits of eighth-order polynomials. (**b**) Effect of the different TARPs on rectification index $RI_{+60/-80}$ of homomeric GluR4 receptors (error bars, s.e.m.; **P < 0.005; ***P < 0.0005; see Supplementary Table 1). (**c**) Representative glutamate-evoked currents at −80 mV and +80 mV for GluR4 alone (left), GluR4 with γ-2 (middle) or GluR4 with γ-5 (right). Currents are scaled to the same peak at −80 mV. Steps beneath each record denote the application of glutamate.
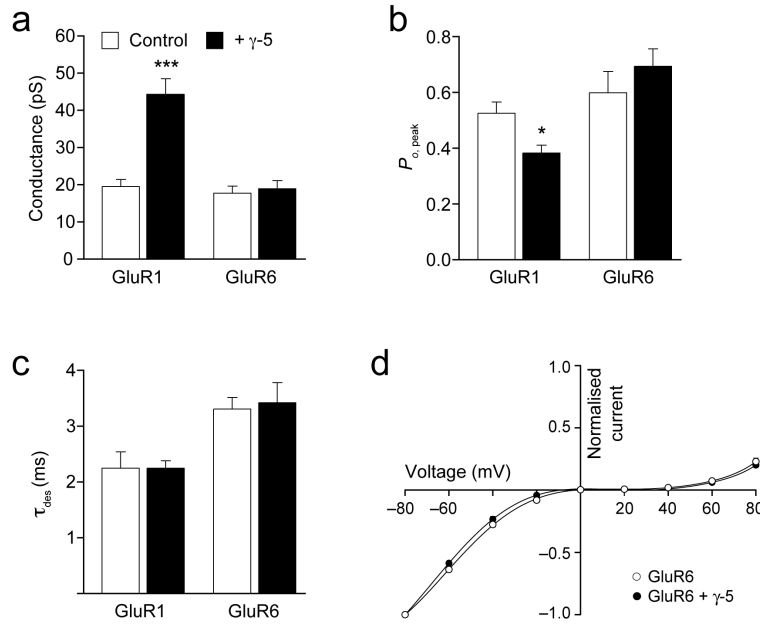
Figure 4. γ-5 modifies the properties of homomeric GluR1 CP-AMPARs but not those of homomeric GluR6 kainate receptors

(**a**) γ-5 increased the channel conductance for homomeric GluR1 receptors but had no effect on conductance of kainate (GluR6) receptors (17.8 ± 1.9 pS without γ-5 versus 18.9 ± 2.2 pS with γ-5; $P = 0.6972$, n = 5 for both). (**b**) γ-5 decreased the open probability ($P_{o,peak}$) of homomeric GluR1 receptors but had no effect on $P_{o,peak}$ of kainate receptors (0.60 ± 0.08 for GluR6, versus 0.69 ± 0.06 for GluR6 plus γ-5; $P = 0.3708$, n = 5 for both). (**c**) γ-5 was without effect on the desensitization time course (τ_{des}) of CP-AMPARs or kainate receptors 3.31 ± 0.20 ms for GluR6, versus 3.42 ± 0.36 for GluR6 plus γ-5; $P = 0.7941$, n = 5). (**d**) Inwardly rectifying I–V relationships for peak currents evoked by glutamate (10 mM, 100 ms) applied to outside-out patches from tsA201 cells containing homomeric GluR6 receptors (n = 7) or GluR6 plus γ-5 (n = 6). Intracellular solution contained 100 mM spermine. Currents are normalized to values at −80 mV; solid lines are fits of eighth-order polynomials. Error bars (s.e.m.) are hidden by symbols. *$P < 0.05$; ***$P < 0.0005$.
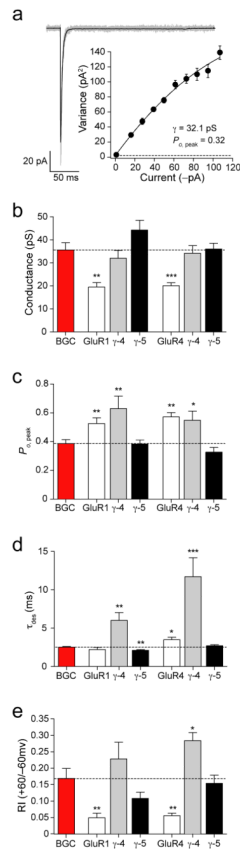
Figure 5. AMPAR responses from BGCs in cerebellar slices suggest a functional role for γ-5
(**a**) Current evoked by rapid application of 10 mM glutamate (100 ms, −60 mV) to an outside-out patch from a BGC in a slice from a P49 mouse. Solid line, the mean of 137 traces; gray line, a representative raw trace. Inset, the current–variance relationship, yielding an estimated weighted mean conductance (g) of 32.1 pS and a $P_{o,peak}$ of 0.32. Dashed line, background variance. (**b–e**) Estimated mean single-channel conductance (**b**), probability of agonist-bound channel opening (peak open probability, $P_{o,peak}$; **c**), kinetics of receptor desensitization (τ_{des}; **d**), and rectification index $RI_{+60/-60}$ (**e**) from BGCs and tsA201 cells expressing GluR1 or GluR4 AMPARs, with and without γ-4 or γ-5. Error bars, s.e.m.; *$P < 0.05$; **$P < 0.005$; ***$P < 0.0005$.
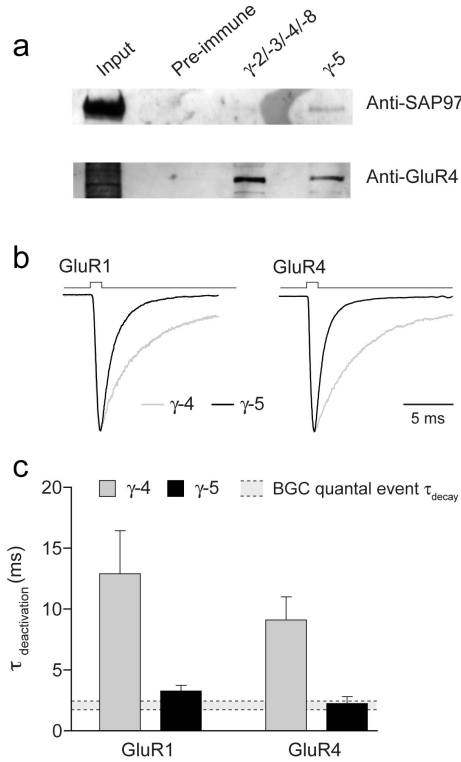
Figure 6. γ-5 differentially affects 'long-form' AMPAR subunits

(**a**) Plot of rectification index (RI) against single-channel conductance (determined using NSFA) for patches from tsA201 cells expressing GluR4 homomeric receptors (filled squares), GluR2/4 heteromeric receptors (open circles) and GluR2L/4 heteromeric receptors (filled circles), with- (red) and without γ-5 (blue). Symbols show mean data (see text for details) and error bars s.e.m. Lines are single exponential fits. Note that for patches with high RI values γ-5 increased conductance only when GluR2L was present (see Table S2). (**b-d**) Comparison of effects of γ-2 and γ-5 on GluR2(Q) and GluR2L(Q) receptors (see Table S3). (**B**) Single-channel conductance for both GluR2(Q) and GluR2L(Q) was increased by co-expression of γ-2, but γ-5 increased the conductance of GluR2L only. (**c**) Peak open probability ($P_{O,\text{peak}}$) of GluR2(Q) and GluR2L(Q) receptors was increased by co-expression of γ-2, but not by γ-5. (**d**) For GluR2(Q), RI was altered by γ-2 but not by γ-5, while for GluR2L(Q) RI was increased both by γ-2 and γ-5. In **b-d**, bars denote mean, error bars s.e.m. and asterisks denote significance (* $P<0.05$; ** $P<0.005$; *** $P<0.0005$).
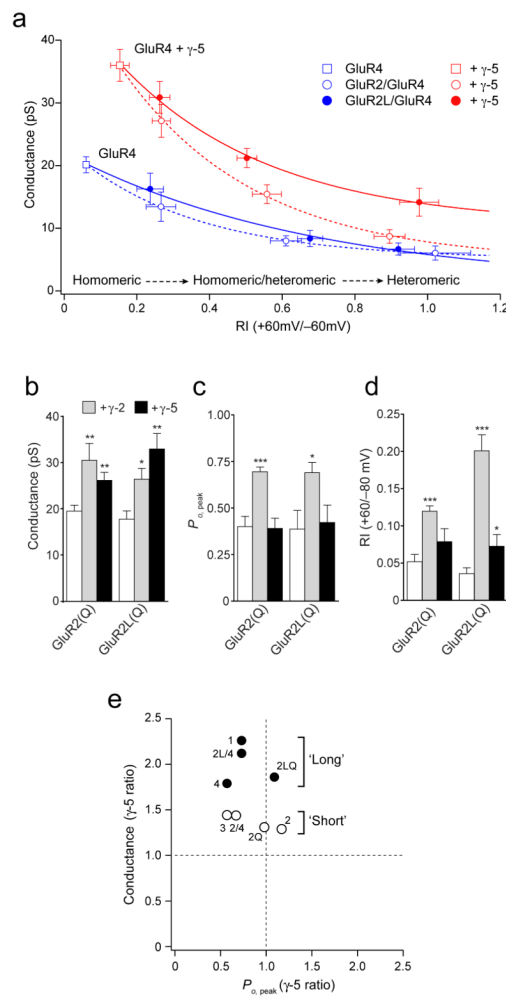
Figure 7. γ-5 interacts with short- and long-form AMPAR subunits but prevents surface expression of short-form AMPARs

(**a**) AMPAR subunits GluR2 and GluR2L co-immunoprecipitate with γ-5. YFP-γ-5 was transfected together with GluR2 or GluR2L in tsA201 cells. YFP-γ-5 protein complexes were immunoprecipitated (IP) with anti-GFP antibody and then Western Blotted using anti-GluR2 (IB; immunoblot). IgG controls were negative. Nearest molecular weight markers are indicated. (**b**) Biotinylation showed that GluR2(Q) surface expression was greatly reduced when it was coexpressed with γ-5. (**c**) Pooled data from biotinylation assays (n=3 repetitions) and corresponding electrophysiological assays (n=6 cells each). Bars denote mean, error bars s.e.m. and asterisks denote significance (* P<0.05; ** P<0.005).
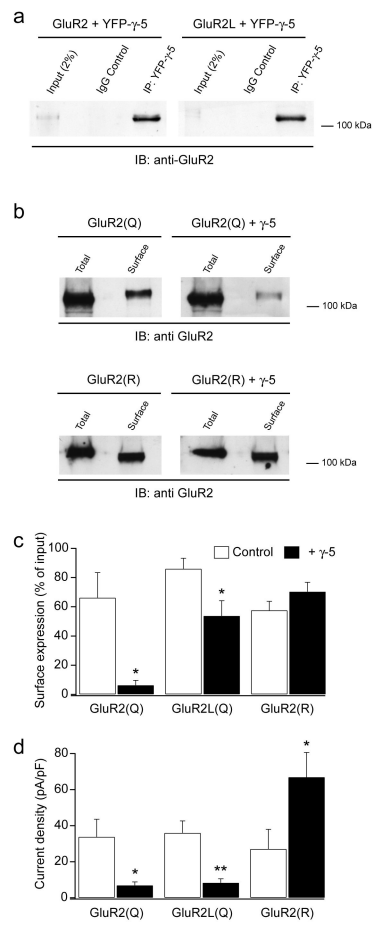
Figure 8.